

## MODELING AND VERIFICATION OF LATERAL BEHAVIOR OF RC FRAME WITH AND WITHOUT INFILL MASONRY

Humayra Adiba Newaz\*<sup>1</sup>, Sadia Mounota<sup>2</sup>, Md. Wahidul Islam<sup>3</sup> and Debasish Sen<sup>4</sup>

<sup>1</sup> Undergraduate Student, Ahsanullah University of Science & Technology, Bangladesh, e-mail: [170103170@aust.edu](mailto:170103170@aust.edu)

<sup>2</sup> Undergraduate Student, Ahsanullah University of Science & Technology, Bangladesh, e-mail: [diasa1141999@gmail.com](mailto:diasa1141999@gmail.com)

<sup>3</sup> Undergraduate Student, Ahsanullah University of Science & Technology, Bangladesh, e-mail: [170103061@aust.edu](mailto:170103061@aust.edu)

<sup>4</sup> Assistant Professor, Ahsanullah University of Science & Technology, Bangladesh, e-mail: [debasish.ce@aust.edu](mailto:debasish.ce@aust.edu)

\*Corresponding Author

### ABSTRACT

Masonry infilled RC frame is very common in developing countries e.g., Bangladesh due to the availability and low cost. In general, contribution of masonry infill is neglected during design of RC building and masonry infills are considered as non-structural element. However, past earthquakes e.g., Nepal EQ 2015 showed that infill masonry can make a difference on the overall behavior of RC frame under seismic load. Hence, assessing the effect of masonry infill for RC Structures responding under seismic loads is of an imminent need for designing the structures more conveniently. Several researchers conducted experiments to see how masonry infill affects the lateral behavior of RC frames. However, it is essential to develop an appropriate methodology to numerically model and accommodate the impact of masonry infill in various commercially available design software, e.g., ETABS, SAP2000, etc. This study aims to model two single bay-single story RC frames, without and with masonry infill, available in literature and simulate lateral behavior with the experimental strength. As per the experimental case study, the models were constructed as such with an intent to simulate the poor materials availability in developing countries. The RC frame i.e., column and beam has been modelled using lumped plasticity approach which is generally employed in various commercially available software for design purpose of multistoried structures such as SAP2000. The columns in both the RC frame and the brick (masonry) infilled reinforced concrete frame were subjected to a continuous axial load of 350 KN. Flexural hinges have been allocated at the endpoints of RC beams and columns (where flexure is likely to fail), whereas shear hinges have been assigned at the mid-height of the columns to adopt the lumped plasticity method. The masonry infill has been idealized as a diagonal strut which is expected to fail by the formation of axial hinge at a specific load that has been calculated based on expected failure mechanism of infill masonry (i.e., diagonal compression or sliding). Both the numerically modeled bare RC frame and the infill masonry RC frame's lateral behavior under seismic response were in good agreement with the experimental lateral behavior. For bare frame and masonry-infilled RC frames, the numerical to experimental lateral capacity ratios are 0.78 and 0.89, respectively.

**Keywords:** Reinforced concrete frame, Masonry infilled reinforced concrete frame, Lateral behavior, Experimental results, Analytical modelling.

### 1. INTRODUCTION

Usage of masonry infilled RC Structures are of the most common type of structures in both developing and under-developed countries such as Bangladesh. During the design of a structure, the contribution of masonry infill in the structure as a load carrying element is neglected but past earthquakes and investigation of several researcher such as Demirel et al. (2017), Seki et al. (2018), Karayannis et al. (2005), Zovkic et al. (2012) etc. indicate that masonry infill can affect the behaviour of RC structures

against lateral or seismic effects. In seismic analysis, the use of non-linear static approaches for evaluating seismic performance of existing structures, as well as design verification of new structures, is becoming more frequent. As a result, understanding the capabilities and limits of the most widely implemented software in design is essential. Different software programs employ various modeling approaches to evaluate a structure's seismic performance. Among several modeling approaches, Finite Element Method (FEM), Distributed Plasticity Model and Lumped Plasticity Model are used for verification.

The Finite element method (FEM) is used to quantitatively solve field problems. Under a variety of loads, FEM accurately calculates the lateral displacement, stresses, and strains of a structure (Oñate, E., 2009). It is primarily used for research. As a result, it is a strong tool for analysis. However, for design reasons, calculating stress-strain extremely precisely is not a key problem. That is why this approach is ignored in this case. The distributed plasticity model, often described as fibre modelling, is a type of distributed plasticity model. This approach is unquestionably one of the more accurate methods of non-linear modelling of RC structures. The obtained axial stress from modelling is directly compared to the maximal concrete compressive strength to determine whether or not it is failing. The same is applicable for reinforcing steels (Taucer, F., Spacone, E., & Filippou, F. C., 1991). Non-linear behaviours or plastic hinges are considered at the endpoints of the structural components in the Lumped Plasticity Model, whereas the body is represented as an elastic portion. This model's assumptions decrease the computational time and storage needs for three-dimensional finite element model results. During the modelling phase, greater emphasis should be placed on the plastic hinge lengths and the description of the inelastic portion. Despite the fact that the distributed plasticity model is far more precise than that of the lumped plasticity model, subsequent investigations have showed no significant difference in the analytical outcomes of both models (Rahai et al., 2013). Instead of the distributed plasticity model, commercial software for the lumped plasticity model is easily accessible. This is why the lumped plasticity model is being used in this study.

The main goal of this work is to compare the lateral behavior of the numerically modelled bare RC frame and infilled (masonry) RC frame based on lumped plasticity modeling by using a commercially widely available software such as SAP2000 to verify whether the maximum base shear capacity within the maximum displacement provides satisfactory results for the numerically modelled frames with non-linear static analysis to the lateral behavior of the frames obtained in a previous study by Seki et al. (2018)

## **2. REFERENCE TEST SPECIMEN**

This study investigates the modelling and analysis of a past investigation of retrofit technologies for masonry infilled frames carried out by Seki et al. (2018) and based on this investigation, the validity of the numerical models is checked. The experimental data and result obtained from that investigation is used here to with the intent of verifying the performance of the numerically modelled bare RC frame and masonry-infilled frame.

### **2.1 Specimen Details**

The reference study was done using 5 specimens in total, but for the intent for this study, the bare frame RC Frame model (S1-F) and masonry infilled RC Frame model (S3-FM) are analysed here. Table 1 summarizes the material parameters of the concrete and rebars employed in these models. Both the models adopted similar dimensions and reinforcement layout as provided in the Figure 1.

Table 1: Concrete and Reinforcing Steel Material Properties (all values are in MPa)

Specimen	Concrete $f_c'$	Masonry $f_m$	Reinforcement					
			$\Phi 8$		$\Phi 10$		$\Phi 12$	
			$f_y$	$f_{ult}$	$f_y$	$f_{ult}$	$f_y$	$f_{ult}$
S1-F (Bare RC Frame)	-	-	-	-	-	-	-	-
S3-FM (Masonry Infilled RC Frame)	14	11.6	364	429	454	553	428	525

Where,  $f_c'$  = concrete compressive strength,  $f_m$  = masonry compressive strength,  $f_y$  = yield strength of reinforcement,  $f_{ult}$  = ultimate strength of reinforcement

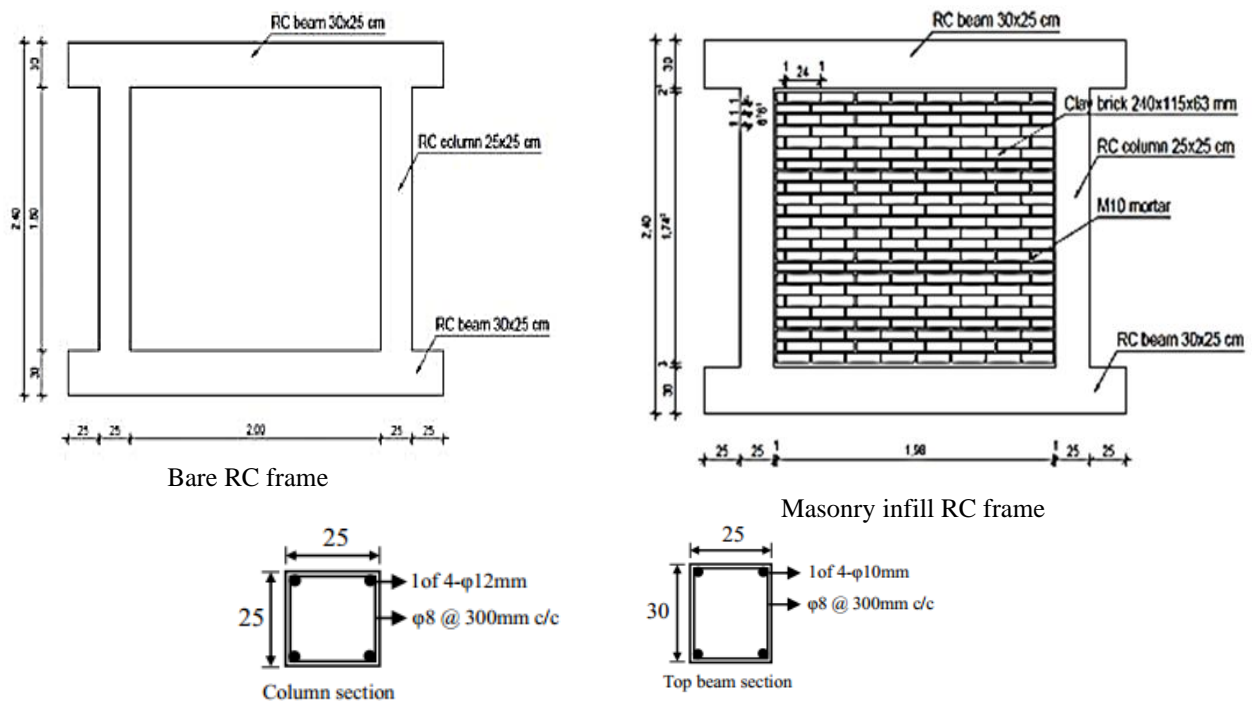


Figure 1: Test Specimens &amp; Dimensions Layout with Reinforcement Details (Seki et al. 2018)

Both reference specimens were subjected to a quasi-static cyclic static lateral stress while being held at a constant axial (vertical) load. Each column was exposed to a steady vertical load of 350 KN, with a cyclic lateral drift of 0.0625 %, 0.125 %, 0.25 %, 0.50 %, 1.0 %, 1.55%, 2.0 %, and 3.0% applied in two cycles for each lateral drift.

## 2.2 Specimen Test Results

The highest measured lateral force up until failure for the bare RC Frame was 81 KN, which corresponded to 1% lateral drift, but the lateral force for the masonry infilled RC Frame was 190 KN, which corresponded to -1 % drift. The damage to the bare Reinforced Concrete frame was localized on the columns, with just a minor break in the beam. The failure of the infilled (masonry) RC frame was caused by formation of flexural hinges at the ends of the column elements subsequently forming shear cracks at the bottom of both the columns, which began with a diagonal tension fracture and progressed to shear slides.

## 3. NUMERICAL MODELING

Both the bare RC frame (S1-F) and masonry infilled RC frame (S3-FM) specimens of the reference test have been modelled in SAP2000 which uses lumped plasticity approach. For the bare RC frame, only

beam & column elements have been used whereas in the case of masonry infilled RC frame, an additional equivalent diagonal strut have been introduced along with the beam & column elements. With the intent of this study, hinges are introduced at specific positions which are discussed here.

### 3.1 Hinge Definition

As lumped plasticity model has been followed, hinges are provided on the points of a structure where it is expected to be cracked or yielded with relatively higher intensity so that under a cyclic loading it shows higher flexural or shear displacements. As a result, hinges are assigned at the beam and column's extreme parts. That is, flexural hinges are assigned at both ends of the beam and column elements, while hinges for shear are assigned in the center of the columns. The indicated flexural and shear hinges on the beam and column components are shown in Figure 3(a). An analogous diagonal strut is introduced in addition to the beam and column components for the masonry infill RC model, and an axial hinge is introduced at the mid height of the diagonal strut, as shown in Figure 3(b).

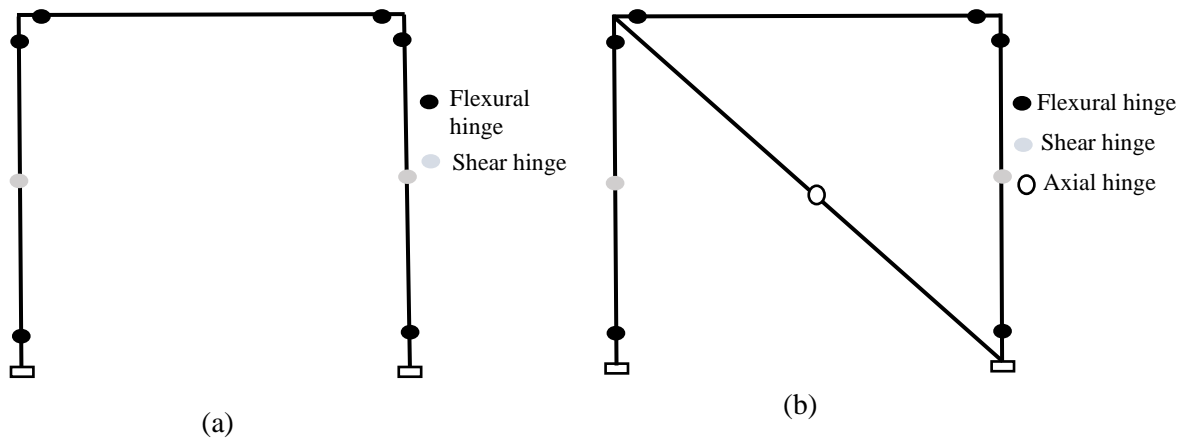


Figure 2: (a) Bare RC Frame with Flexural & Shear hinge (b) Masonry Infilled RC Frame with Flexural, Shear and Axial hinge

#### 3.1.1 Flexural Hinge (For Beam and Column)

Flexural hinges reflect the instantaneous rotating connection of the beams and columns. It is inserted at both the beam and the column ends. The following curve depicted in Figure 4 represents the typical deformation regulated hinge behavior with an elastic range from point 0 to 1 and a plastic zone spanning points 1 to 3. At point 3, the plastic range is characterised by significant residual strength and the capacity to withstand gravity loads. Because of this sort of behavior, the model was deformation-controlled. The plastic range contains a strain hardening range of points 1 to 2 and a strength-degraded range of points 2 to 3. (FEMA 356).

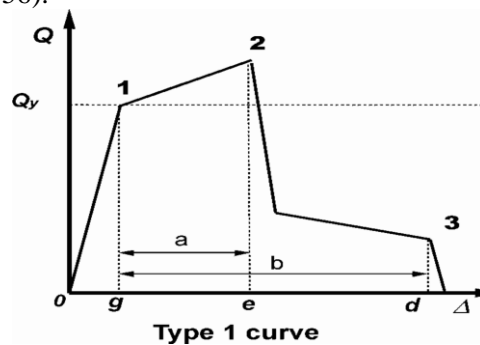


Figure 3: Component Force vs. Deformation Curve for flexure (FEMA 356, 2000)

According to the formula proposed by the JBDPA seismic evaluation guideline (2001), the ultimate flexural strength of columns shall be calculated as equation (1). Yield strength of both beam and column ( $M_y$ ) is taken as the divisor of 1.1 of the ultimate strength of both beam and column ( $M_u$ ) respectively. The beam ultimate flexural strength must be calculated as equation (2).

For  $0.4 * D * F_c \geq N \geq 0$ ;

$$M_u = (0.8a_t * \sigma_y * D) + 0.5N * D * \left[ 1 - \left\{ \frac{N}{b * D * F_c} \right\} \right] \quad (1)$$

$$M_b = 0.9 * a_t * \sigma_y * d \quad (2)$$

Where,  $N$  = Axial force (N),  $a_t$  = Tensile reinforcing bars' total cross-sectional area ( $\text{mm}^2$ ),  $b$  = Width of the column (mm),  $D$  = Column Depth (mm),  $\sigma_y$  = Reinforcing bar yield strength ( $\text{N}/\text{mm}^2$ ),  $F_c$  = Concrete compressive strength ( $\text{N}/\text{mm}^2$ ),  $d$  = effective depth of the beam.

### 3.1.2 Shear Hinge

The sliding failure of the beam and columns is represented by a shear hinge. In this model, shear hinge on beam is ignored as it is unlikely that the beam will fail under shear as both the bare RC frame and masonry infilled RC frame of the reference test showed concentrated failure in columns. The shear hinge is assigned as force controlled (brittle). The component shear force vs deformation curve will act as shown in Figure 5, described in FEMA 356: where the elastic range is 0 to 1 on the curve and the plastic range is 1 to 2 on the curve, followed by a loss of strength and capacity to resist gravity loads beyond point 2, signifying abrupt failure.

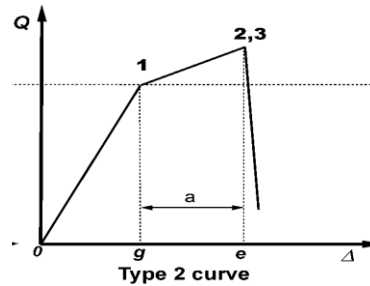


Figure 4: Component Force Vs Deformation Curve for Shear (FEMA 356, 2000)

According to the formula proposed by the JBDPA seismic evaluation guideline (2001), columns ultimate shear strength must be determined as equation (3):

$$Q_{su} = \left\{ \frac{\{ (0.053\rho_t^{0.23} (18+F_c) \}}{M/Q + 0.12} + 0.85\sqrt{\rho_w * s\sigma_{wy}} + 0.1\sigma_0 \right\} * b * j \quad (3)$$

Where,  $\rho_t$  = Ratio of tensile reinforcement (%),  $\rho_w$  = Ratio of shear reinforcement, ( $\rho_w = 0.012$  for  $\geq \rho_w$  0.012)  $s\sigma_{wy}$  = Shear reinforcing bar yield strength ( $\text{N}/\text{mm}^2$ ),  $\sigma_0$  = Axial column stress ( $\text{N}/\text{mm}^2$ ),  $d$  = D-50mm may be used as the column's effective depth.,  $M/Q$  = The length of a shear span and  $h_o/2$  is the default value.,  $h_o$  = The column's clear height,  $j$  = The default value for the distance between the centroids of tensile and compressive forces is 0.8D.

### 3.1.3 Axial Hinge

At the midpoint of the diagonal strut, an axial hinge is placed which is inserted at the mid-height of the diagonal strut, which is force-controlled. The deformation behavior for the axial force in Figure 6 was also described graphically in FEMA 356 (2001). The curve represents brittle or nonductile performance, with an elastic range from point 0 to point 1 on the plotted curve, subsequently followed by a reduction in strength and ability to withstand axial loads exceeding point 1, with failure occurring immediately after reaching the ultimate capacity.

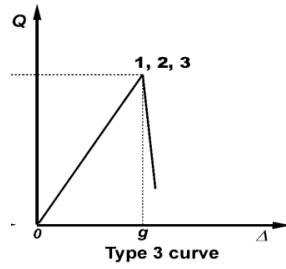


Figure 5: Component force vs Deformation Curve for Axial Capacity (FEMA 356, 2000)

The elastic in-plane rigidity of both a solid unstrengthened infill masonry panel prior to cracking is represented by a diagonal compression strut. The lateral capacity of equivalent masonry infill strut will be considered as the minimum of the diagonal compression capacity and sliding capacity as indicated in equation (4). The sliding capacity of the infill strut  $P_{strut(S)}$  was calculated according by the proposal of Paulay & Priestly (1992) using equation (5) and the diagonal compression strut capacity was calculated utilizing equation (6) where the width of the infilld strut,  $a$  is calculated using equation (7) along with the Coefficient used to determine equivalent width of infill strut  $\lambda_1$  as per equation (8).

$$Q_{strut} = \min \{ (P_{strut(DC)} \& P_{strut(s)}) \} \quad (4)$$

$$P_{strut(s)} = \left\{ \left( \frac{0.03 * f_m}{1 - \mu \frac{h_{inf}}{L_{inf}}} \right) * (L_{inf} * t_{inf}) \right\} * \frac{1}{\cos \theta} \quad (5)$$

$$P_{strut(DC)} = a * t_{inf} * \frac{f_m}{2} \quad (6)$$

$$a = 0.175 (\lambda_1 * h_{col})^{-0.4} r_{inf} \quad (7)$$

$$\lambda_1 = \left[ \frac{E_{me} t_{inf} \sin 2\theta}{4 E_{fe} I_{col} h_{inf}} \right]^{\frac{1}{4}} \quad (8)$$

Where,  $E_{me}$  = expected modulus of elasticity of the material of the infill =  $550 \times f_m$ ,  $f_m$  = Masonry compressive strength,  $t_{inf}$  = Thickness of infill panel & diagonal strut,  $h_{col}$  = column height between the centerlines of beam,  $h_{inf}$  = height of infill panel,  $E_{fe}$  = expected modulus of elasticity of the material of the frame,  $I_{col}$  = moment of inertia of column,  $L_{inf}$  = length of masonry infill panel,  $r_{inf}$  = diagonal length of masonry infill panel.

### 3.2 Hinge Assignment

The discussed flexural, shear and axial hinges are assigned at the specific positions presented in Figure 3. The hinge property is dependent upon the yield moment (for deformation-controlled) or the shear/axial force (for force-controlled). The values of these parameters were calculated as per JBDPA seismic evaluation guideline (2001) and FEMA 356 (2000) as mentioned previously which was then input in SAP2000.

The calculated Ultimate Flexural Strength for column using equation (1) was found at 45.613 KN-m and subsequently the yield strength was found at 41.466 KN-m. For beam, the ultimate flexural strength using equation (2) was found at 16.367 KN-m and the yield strength was found at 14.879 KN-m. Both the data of yield strength was input in SAP2000 as hinge property data accordingly which are presented in Figure 7(a) and 7(b). The calculated ultimate shear strength of the column using equation (3) was found at 79.17 KN which was then input as hinge property data in SAP2000 which is presented in Figure 7 (c). The calculated strut capacity along the axial direction using equation (10) was found at 147.54 KN which was then input at SAP2000 as shown in figure 7(d).

Frame Hinge Property Data for column - Moment M3

Edit

Displacement Control Parameters

Point	Moment/SF	Rotation/SF
D	-0.2	-0.025
C	-1.1	-0.015
B	-1	0
A	0	0
C	1.1	0.015
D	0.2	0.015
E	0.2	0.025

Load Carrying Capacity Beyond Point E  
 Drops To Zero  
 Is Extrapolated

Scaling for Moment and Rotation  
 Use Yield Moment Moment SF 41.456  
 Use Yield Rotation Rotation SF 1

Acceptance Criteria (Plastic Rotation/SF)  
 Immediate Occupancy 3.000E-03  
 Life Safety 0.012  
 Collapse Prevention 0.015

OK Cancel

(a)

Frame Hinge Property Data for beam - Moment M3

Edit

Displacement Control Parameters

Point	Moment/SF	Rotation/SF
D	-0.2	-0.025
C	-1.1	-0.015
B	-1	0
A	0	0
C	1.1	0.015
D	0.2	0.015
E	0.2	0.025

Load Carrying Capacity Beyond Point E  
 Drops To Zero  
 Is Extrapolated

Scaling for Moment and Rotation  
 Use Yield Moment Moment SF 14.873  
 Use Yield Rotation Rotation SF 1

Acceptance Criteria (Plastic Rotation/SF)  
 Immediate Occupancy 3.000E-03  
 Life Safety 0.012  
 Collapse Prevention 0.015

OK Cancel

(b)

Frame Hinge Property Data for shear hinge - Shear V2

Force Control Parameters

Maximum Allowed Force  
 Specified Proportion of Yield Force  
 User Specified Force  
 Positive: [ ] Negative: [ ]  
 Positive: 79.17 Negative: [ ]

Hinge Loses All Load Carrying Capacity When Maximum Force Is Reached

Acceptance Criteria (Force/Maximum Allowed Force)  
 Immediate Occupancy 0.5  
 Life Safety 0.8  
 Collapse Prevention 1

Hinge is Symmetric (Tension Behavior Same as Compression Behavior)

OK Cancel

(c)

Frame Hinge Property Data for strut - Axial P

Force Control Parameters

Maximum Allowed Force  
 Specified Proportion of Yield Force  
 User Specified Force  
 Positive: [ ] Negative: [ ]  
 Positive: 2.000E-09 Negative: -147.54

Hinge Loses All Load Carrying Capacity When Maximum Force Is Reached

Acceptance Criteria (Force/Maximum Allowed Force)  
 Immediate Occupancy 0.5  
 Life Safety 0.8  
 Collapse Prevention 1

Hinge is Symmetric (Tension Behavior Same as Compression Behavior)

OK Cancel

(d)

Figure 6: (a) Flexural Hinge Property Data of Column; (b) Flexural Hinge Property Data of Beam; (c) Shear Hinge Property Data of Column. (d) Axial Hinge Property Data of Masonry Infill Strut

### 3.3 Load Definition

According to the reference test specimen, 350 KN loads as gravity load was input in each column vertically. For the case of horizontal loading, the lateral load case was generated by employing UBC 94 default standard. And as this modelling employs non-linear static analysis i.e, pushover analysis, the pushover case was generated such that the loading condition starts from the effect of gravity load.

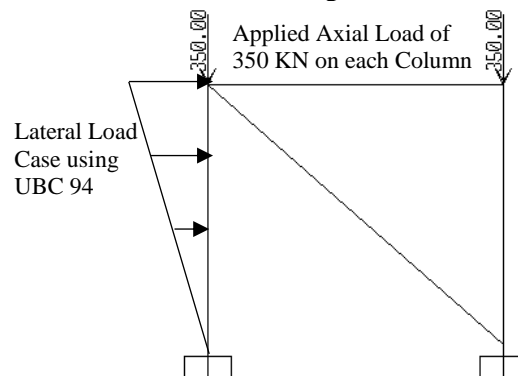


Figure 7: Axial load 350KN is applied on each column modeled on SAP2000.

#### 4. EVALUATING THEORETICAL CAPACITY

The theoretical capacity of the frame is calculated using the JBDPA seismic evaluation (2001) criteria and FEMA356.

##### 4.1 Bare Frame Capacity

The theoretical lateral capacity of the bare RC frame will be taken to be twice the minimum flexural or shear capacity as per equation (9). The flexural capacity and shear capacity are evaluated using the JBDPA seismic evaluation guideline (2001). The Flexural capacity  $Q_{mu}$  will be obtained using equation (10) and the shear capacity to be obtained is described previously in equation (3).

$$Q_{bf} = 2 * (\min. \text{ of } Q_{mu}, Q_{su}) \quad (9)$$

$$Q_{mu} = \frac{2M_u}{h_o} \quad (10)$$

Where,  $Q_{mu}$  = Ultimate flexural strength,  $Q_{su}$  = Ultimate shear strength,  $M_u$  = Ultimate Moment of the columns,  $h_o$  = Clear height of the column.

##### 4.2 Masonry Infill Capacity

The lateral capacity of masonry infill,  $Q_{strut}$  will be considered as the minimum of diagonal compression strut capacity or sliding strut capacity in the horizontal direction component,  $Q_{strut} \cos \theta$  utilizing equation (4). The sliding strut capacity is calculated as described in equation (5) is and the diagonal compression strut capacity is calculated described in equation (6).

#### 5. ANALYSIS AND RESULTS

The numerical results obtained from the pushover capacity curve of SAP2000 were compared with experimental and theoretical results.

##### 5.1 Comparison of Numerical Results With Experimental & Theoretical Results

Pushover analysis is a static approach that uses a basic, non-linear technique to estimate seismic structural deformation. The capacity, or "pushover" curve, of a building is the base shear force versus the horizontal roof displacement curve that describes the load displacement of a structure. After assigning all of the loads and hinges to the bare frame and masonry infill RC frame models, pushover analysis using SAP2000 is performed. The pushover curves for the bare RC frame and the masonry infill RC frame are shown in Figures 9(a)-(b).

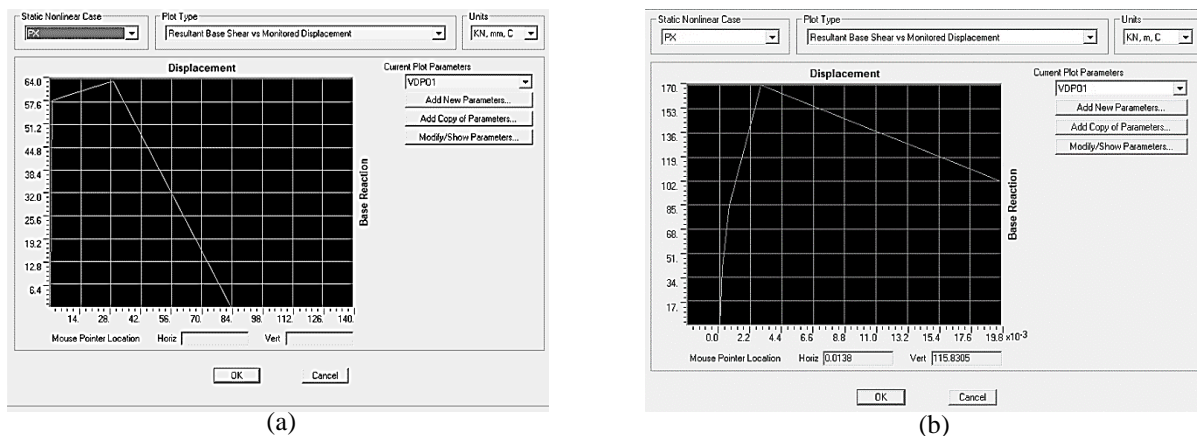


Figure 8: (a) Pushover Curve for Bare RC Frame; (b) Pushover curve of masonry infill RC frame.

It shows that the capacity for the bare RC frame is 63.43 KN and for the masonry-infilled RC frame is 169.83 KN, which indicates that after putting the masonry infill, the capacity rises by a significant amount. According to SAP2000, the total capacity ratio between masonry-infilled RC frame and bare frame is 2.68, while the experimental ratio is 2.35. Table 2 summarizes the capacities determined from the SAP2000 pushover curves for bare RC frames and masonry-infilled frames. The calculated capacities of the bare frame at 63.58 KN and the infilled frame at 173.26 KN show similarity to the capacities obtained from SAP2000, with the bare frame capacity being 63.43 KN and the infilled frame capacity being 169.83 KN, which means that the calculations are almost identical as compared to the capacities from SAP2000. From table 2, it is seen that the SAP2000 to experimental has a bare frame capacity ratio of 0.78, whereas theoretical to experimental has a ratio of 0.785, which is nearly equal. The brick infill RC frame capacity ratio between SAP2000 and experimental is 0.89, and the theoretical to experimental ratio is 0.91, which is also nearly similar.

Table 2: Summary of Evaluated Lateral Capacity

Frame Type	Component (All capacities are expressed in kN)	Specimen	
		Bare Frame	RC Frame with Masonry Infill
RC Frame	Lateral Capacity, Q as equation (9)	63.58	63.58
Masonry Infill Strut	Diagonal Compression Capacity as equation (6)	-	134.09
	Sliding Capacity as equation (7)	-	109.68
Total Calculated Capacity		63.58	173.26
Experimental Capacity		81	191
Capacity obtained from SAP2000		63.43	169.83
Predicted (SAP2000)/Experimental		0.78	0.89
Predicted (Theoretical)/Experimental		0.78	0.91

## 5.2 Numerical Behavior of Models

Due to the brittle behavior of masonry brick, the ductility of the bare RC frame decreases with the insertion of masonry infill. When the masonry cracks, there is a rapid decrease in stiffness and maximum load in the infilled frame. So, the axial force of the column elements decreases with the insertion of masonry infill. The axial force of the masonry infill RC frame at peak resistance is less than the axial force of the bare frame, as shown in Figure 10(b). As the axial force of the column elements decreases, the bending moment of the bare frame also decreases with the insertion of masonry infill. However, as shown in figure 10(b), the beam has some axial loads that are nearly absent in the case of the bare RC frame shown in figure 9(b), which is due to the horizontal component of the diagonal strut. The bending moment of the masonry infill RC frame at peak resistance is 41.69 KN, which is less than the bending moment of the bare frame, which is 45.42 KN, as shown in Figure 10 (a). And hinges are formed where the bending moment is at its maximum. Figure 9(c) shows that hinges are formed at the end of the beam and at the bottom of the column, where the bending moment is greatest, as shown in figure 9(a). And in the diagonal strut, the hinge is formed at the mid length of the column. The bare RC frame reaches its peak at step 7. At this step, both the columns fail, and the masonry-infilled RC frame reaches its peak at step 4. At this step, the axial hinge assigned to the infill strut reaches to life safety from immediate occupancy, which means the strut only failed but the columns did not. This is also shown in figures 9(a) and 10(a), where the bending moment of the column elements for bare RC frames is 45.42 kN-m, whereas for an infilled RC frame, the bending moment of the column elements is 41.69 kN-m.

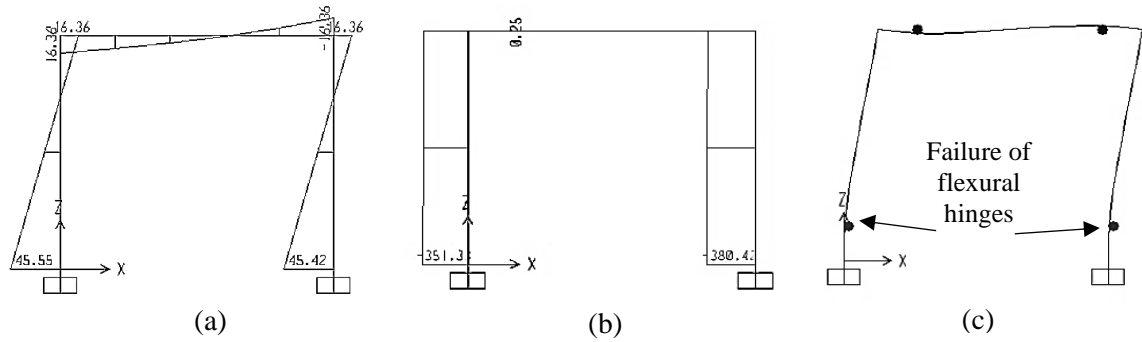


Figure 9: (a) Bending Moment Diagram (kN-m); (b) Axial Force Diagram (kN); (c) Hinge Locations at critical points of Bare RC Frame at peak resistant

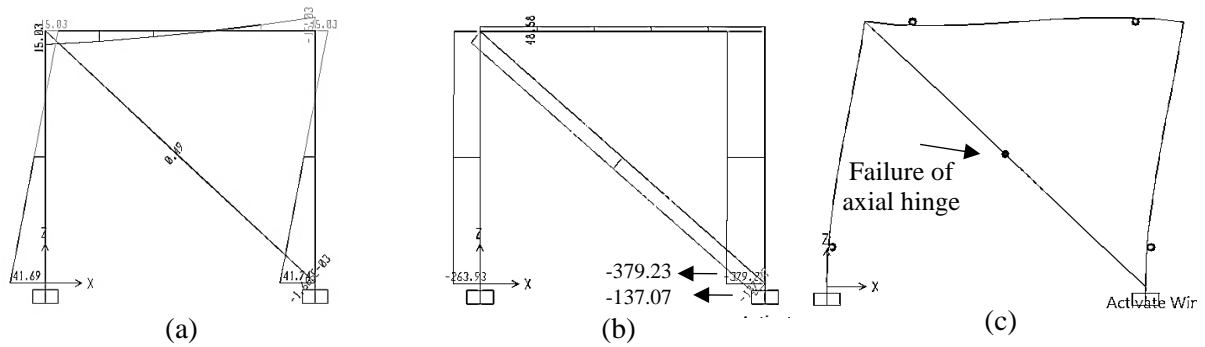


Figure 10: (a) Bending Moment (kN-m) Diagram; (b) Axial Force Diagram (kN); (c) Hinge Formation Locations at critical points of RC Frame with Masonry Infill

## 6. CONCLUSIONS

In this study, the lateral capacity of a bare frame and a masonry-infilled RC frame is evaluated. A numerical model has also been developed using the lumped plasticity modeling approach in SAP2000. It is observed that,

- For bare frame and masonry-infilled RC frames, the numerical to experimental lateral capacity ratios are 0.78 and 0.89, respectively.
- The installation of masonry infill has also been shown to increase the bare frame lateral capacity. According to SAP2000, the total capacity ratio between masonry-infilled RC frame and bare frame is 2.68, while the experimental ratio is 2.35. Masonry infill influences the seismic performance of an RC frame structure by improving the overall strength of the structure.

## REFERENCES

- Demirel, İ. O., Yakut, A., & Binici, B. (2017, January). Seismic behaviour of RC frames infilled with different techniques. In *16th World Conference on Earthquake Engineering* (pp. 9-13)
- FEMA 356. (2000). American Society of Civil Engineers for the Federal Emergency Management Agency. *Prestandard and commentary for the seismic rehabilitation of buildings*.
- JBDPA (Japan Building Disaster Prevention Association). (2001). *Guideline for post-earthquake damage evaluation and rehabilitation*. Tokyo: JBDPA (Japan Building Disaster Prevention Association)
- Karayannis, C. G., Kakaletsis, D. J., & Favvata, M. J. (2005). Behavior of bare and masonry infilled R/C frames under cyclic loading: experiments and analysis. *WIT Transactions on The Built Environment*, 81.

- Oñate, E. (2009). Introduction to the finite element method for structural analysis. *Structural analysis with the finite element method: linear statics*, 1-42.
- Paulay, T., & Priestley, M. N. (1992). *Seismic design of reinforced concrete and masonry buildings*. New York: Wiley.
- Rahai, A. R., & Fallah Nafari, S. (2013). A comparison between lumped and distributed plasticity approaches in the pushover analysis results of a pc frame bridge. *International Journal of Civil Engineering*, 11(4), 217-225.
- Seki, M., Popa, V., Lozinca, E., Dutu, A., & Papurcu, A. (2018). Experimental study on retrofit technologies for RC frames with infilled brick masonry walls in developing countries. *Proceedings of the 16th ECEE, Romania*.
- Taucer, F., Spacone, E., & Filippou, F. C. (1991). *A fiber beam-column element for seismic response analysis of reinforced concrete structures* (Vol. 91). Berkeley, California: Earthquake Engineering Research Center, College of Engineering, University of California.
- Zovkic, J., Sigmund, V., & Guljas, I. (2013). Cyclic testing of a single bay reinforced concrete frames with various types of masonry infill. *Earthquake engineering & structural dynamics*, 42(8), 1131-1149.